# The Feasibility of Measuring Lung Hyperinflation With a Smart Shirt: An in Vitro Study

Denise Mannée, Hanneke van Helvoort, and Frans de Jongh

***Abstract*—Home monitoring of patients with chronic obstructive pulmonary disease can increase quality of life and decrease health care costs. Despite the existence of an important relationship between lung hyperinflation (LH) and patient outcomes, LH is often ignored in home monitoring as it difficult to assess at home. A smart shirt containing respiratory inductance plethysmography (RIP, which measures thoracic and abdominal cross-sectional area changes) is a promising tool for home monitoring of LH. This study investigates the feasibility of a smart shirt to monitor LH. We aimed to describe the relationship between temperature and the output, and between the circumference and output of the smart shirt and to correct for temperature dependency. To do so, the smart shirt was applied to a custom-made torso model. Ambient temperature was increased and decreased in 15 tests, while maintaining a constant torso circumference to derive a temperature correction. Additionally, sensor output was monitored with varying circumference. The results revealed a linear relation between temperature and RIP output. Nine of the twelve shirts showed a linear output to changes in circumference. A median temperature drift of −34.7 mL/°C was observed and corrected to a minimum drift of −0.5 mL/°C. In conclusion, RIP is a promising method for measuring LH in home monitoring. Patients will not be falsely diagnosed with LH due to temperature changes. Sensor output can easily be corrected for temperature. Furthermore, the relationship between circumference and output is linear, confirming the ease of implementing the calibration procedure for obtaining lung volumes.**

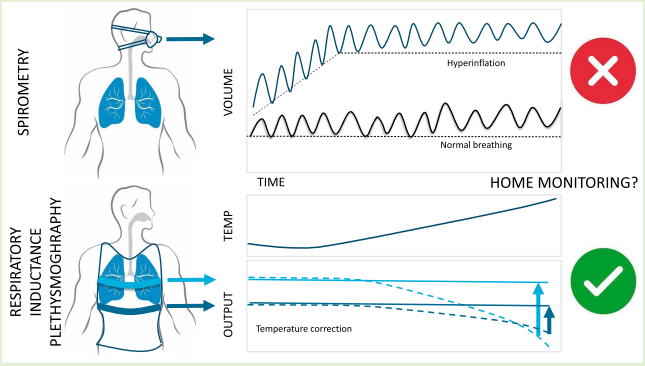


***Index Terms*—Feasibility, lung hyperinflation, respiratory inductance plethysmography, smart shirt, temperature, chronic obstructive pulmonary disease.**

## I. Introduction

CHRONIC obstructive pulmonary disease (COPD) is a common chronic disease caused by prolonged exposure to noxious/toxic particles or gases [1]. The main symptoms of COPD are dyspnoea, coughing and production of sputum. Inflammatory reactions in the lungs of COPD patients cause an increased airway resistance and lung compliance. As a result, airflow is limited, and the lungs are hyperinflated during increased ventilatory demand due to air trapping. [1], [2] Acute exacerbations are defined as an increase of respiratory requiring additional treatment, and may lead to hospitalization [1]. Acute exacerbations have a significant impact on quality of life of patients and lead to an increase in healthcare costs. For this reason, early detection of exacerbations and symptoms of COPD is paramount. To enhance early deterioration of the disease home-based self-management is an important focus for research. Telemonitoring appears to have a positive effect on quality of life, reducing the rate and severity of exacerbations as well as the number of hospitalizations [2]–[6].

Home-monitoring with use of smart textiles is rapidly increasing in health care and in the field of COPD. In smart textiles, conductive fabric and/or sensors are combined with for example shirts or straps. The combination of (bio)-potential sensors with clothes provides the user with daily physiological parameters. These parameters can be assessed continuously, and information can be extracted on a personalized level with use of algorithms [7]–[9]. The smart systems are used in numerous applications, for example in monitoring vital signs [10]–[13], and stress [14]–[17].

Home-monitoring parameters that are currently measured in COPD patients are largely limited to daily measurements of airway obstruction (in terms of expiratory flow) and subjective

Manuscript received June 11, 2020; revised July 9, 2020; accepted July 9, 2020. Date of publication July 20, 2020; date of current version November 18, 2020. This work was supported by the Europees Fonds voor Regionale Ontwikkeling (EFRO). The associate editor coordinating the review of this article and approving it for publication was Prof. Subhas C. Mukhopadhyay. *(Corresponding author: Denise Mannée.)*

Denise Mannée and Hanneke van Helvoort are with the Department of Pulmonary Diseases, Radboudumc, 6500 HB Nijmegen, The Netherlands (e-mail: denise.mannee@radboudumc.nl).

Frans de Jongh is with the Department of Engineering Fluid Dynamics, University of Twente Faculty of Engineering Technology, 7522 NB Enschede, The Netherlands.

This article has supplementary downloadable material available at https://ieeexplore.ieee.org, provided by the authors.

Digital Object Identifier 10.1109/JSEN.2020.3010265

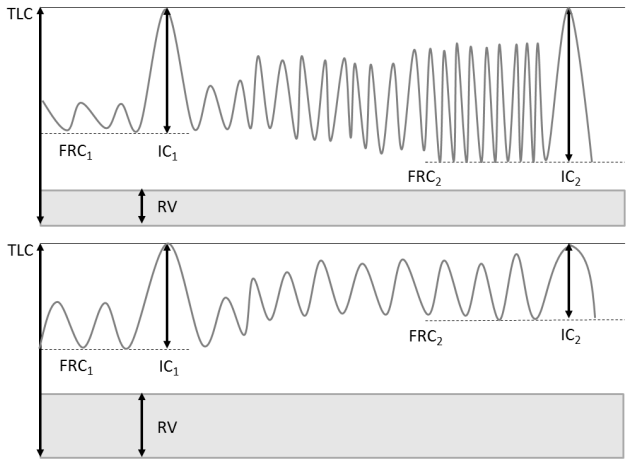


Fig. 1. Breathing pattern of a healthy subject (upper chart) and a COPD patient (lower chart), indicating total lung capacity (TLC), inspiratory capacity (IC), residual volume (RV), and functional residual capacity (FRC).

symptom description [18], [19]. Stenzler [20] suggested that lung volume measurements provide more valuable information on treatment response of COPD patients and may predict occurrence of exacerbations and mortality. [21], [22] Patient outcome could be improved further by measuring additional parameters. Additional parameters that are addressed in the study of Bellos *et al*. [23] include vital signs to assess the health status of COPD patients. Some studies include the daily measurement of lung resistance [24], whereas others add the continuous measurement of multiple respiratory variables (e.g. respiratory rate and oxygen saturation) [25]. Despite the existence of an important relationship between parameters describing lung hyperinflation (LH) and patient outcomes, these parameters are often ignored. [20], [22], [26], [27].

The most important parameter describing LH is functional residual capacity (FRC), which is defined as the amount of air in the lungs after relaxed exhalation [27]. At FRC there exists an equilibrium between the outward force of the chest wall and the inward force of the lungs [28]. The difference between the lung volumes of healthy subjects (a) and COPD patients (b) is visualized in Fig. 1. As a result of increased lung compliance, COPD patients exhibit an increased FRC (i.e. static hyperinflation (SH); see white area in Fig. 1). Moreover, in situations with increased ventilatory demand, a dynamic component of hyperinflation (DH) can occur in patients. DH is a reversible increase in FRC, primarily due to a mismatch between the available and necessary expiratory time. During exercise (grey area), ventilatory demand increases. Healthy subjects exhibit a decrease in FRC (resulting from the use of expiratory muscles), while COPD patients exhibit an increase in FRC due to the failure to exhale fully [27].

The methods currently used to measure SH are body plethysmography and gas dilution which can only be performed in a clinical setting [29]. DH is measured by assessing the inspiratory capacity (IC) during exercise tests or metronome paced tachypneu while subjects were a mask [20], [30]–[33]. Home measurement of DH has three disadvantages. First, the patient must perform unsupervised maximal breathing (IC). Second, the measurements interfere with activities of daily living. Third, with this method the assessment of DH requires using a mask equipped with a flow sensor. An alternative method could potentially overcome these problems [34]–[38].

Respiratory inductance plethysmography has a long history in the respiratory field [39]–[41]. RIP could be a feasible method for measuring DH and SH. This method uses chest wall movements to assess lung volume. It is known that lung volume can be closely approximated by a linear function based on changes in the circumference of the thorax and the abdomen [42]. The change in circumference of the torso of a human subject has a near constant proportional relation to the change in its cross-sectional area. Since the early 1960s RIP has been used extensively in clinical practice for monitoring respiratory parameters during exercise [43]–[45], sleep [40], [46], and mechanical ventilation [47], [48]. Respiratory parameters (e.g. tidal volume and respiratory rate) can be measured accurately compared to traditional methods [39], [43], [49], [50]. Studies that have utilized RIP to measure SH and DH show promising results. In two studies FRC is measured with good accuracy although precision is lacking [51], [52]. In a study by Neumann *et al*. [51] FRC is measured with multiple breath nitrogen washout in unison with RIP, leading to a mean deviation of 11.6 mL (SD: 174.1 mL). Temperature change is identified as a confounding factor for these measurements in both studies.

Temperature changes can cause oscillator drift in RIP technology [53]–[55]. Drift is the gradual movement from an original position and in this case a change in central frequency over time [56]. (most) Oscillators use analog and/or digital high pass filters for this reason. No high pass filters can be applied when measuring such forms of physiological drift (i.e. change in volume over time) as SH and DH, as doing this would filter the parameters of interest. Our initial measurements in healthy subjects wearing a smart shirt containing RIP technology indicated unphysiological signal drift originating from temperature changes in the oscillator within the device.

The main motivation of our study is to develop a tool to measure LH at home to increase patient comfort and decrease health care costs. In the current study the first steps towards home monitoring will be made by trying to establish the relationship between temperature and both the thoracic and abdominal output in arbitrary units (AU) of the smart shirt in vitro. For a linear calibration function to be applicable, the thoracic and abdominal band should have a linear response to changes in circumference. We therefore studied the relationship between the circumference and the output of the shirt. Finally, we endeavored to correct for possible temperature dependency.

## II. Methods

### A. Materials

In RIP technology a voltage-controlled oscillator (Colpitts oscillator) is used to detect changes in cross sectional area of the torso. The oscillator consists of an inductor and two capacitances in series (forming the tank circuit), and an amplifier in the feedback loop. The system is characterized by

TABLE I
AVAILABLE SIZES HEXOSKIN SHIRTS WITH CIRCUMFERENCE RANGE

| Shirt size | Thoracic circumference range | Abdominal circumference range |
|---|---|---|
| F-L (1) | 83 – 91 cm | 78 – 88 cm |
| F-XL (1) | 86 – 94 cm | 84 – 94 cm |
| M-S (1) | 82 – 93 cm | 82 – 93 cm |
| M-2XL (1) | 107 – 118 cm | 107 – 118 cm |
| M-3XL (4) | 114 – 127 cm | 114 – 127 cm |
| M-4XL (4) | 122 – 137 cm | 122 – 137 cm |

M and F refer to shirts for males and females, respectively, with the number of shirts indicated in parentheses. Minimum and maximum thoracic and abdominal circumference (as provided by Hexoskin) are presented in the middle and last columns, respectively.

a central frequency or "oscillator-resonance frequency" ($f_0$). This frequency can be calculated using the reactance of the capacities and inductor. See (1), in which L is the inductance, C1 and C2 are the capacitances, and $f_0$ is the central frequency:

$$f_0 = \frac{1}{2\pi\sqrt{L\frac{C_1C_2}{C_1+C_2}}} \quad (1)$$

In RIP, the inductor is formed by a single coil winding around the thorax and/or abdomen. During breathing, the cross-sectional area of the coil changes, resulting in a change of inductance and a deviation from the central frequency. This deviation can be measured by frequency demodulation of the system [57]–[59].

The Hexoskin smart shirt (Carré Technologies, Montreal, Canada) is a commercially available patented [60]–[62] tool with incorporated sensors; RIP sensors, temperature sensors, electrocardiogram (ECG) sensors and accelerometers. The shirt is made of elastic material which makes it easy to wear and therefore it does not interfere with daily activities. When the shirt is coupled to a "Hexoskin smart device", the device gathers the data from the various sensors and sends them via Bluetooth to a smartphone or tablet. The RIP, temperature and ECG sensors and accelerometers measure with different sample frequencies of respectively 128 Hz, 128 Hz, 256 Hz and 64 Hz. Based on the algorithm developed by Carré Technologies, minute-to-minute data (e.g. heart rate, breathing frequency, minute ventilation, activity intensity) can be derived from the shirt. In various studies the accuracy of the minute-to-minute data has been proven. Breathing frequency was proven to be accurate compared to standard lab methods [63]–[65] as were other respiratory parameters such as maximal oxygen uptake [66] and inspiratory/expiratory time [67]. In other clinical studies, the ECG sensors were confirmed to be an accurate measurement tool for heart rate [65], [68]. Burned calories based on acceleration could be reliably estimated [63].

In this study raw data was used and processed according to our own methods.

The Hexoskin is available in various sizes (see Table I) [69]. In this article, we us abbreviations to refer to specific variants of the shirts. More specifically, M and F are used to refer to shirts for males and females, respectively. This designation is combined with the size of the shirt to indicate the different shirts. The numbers of shirts of each variant that were used in the present study are presented in Table I.

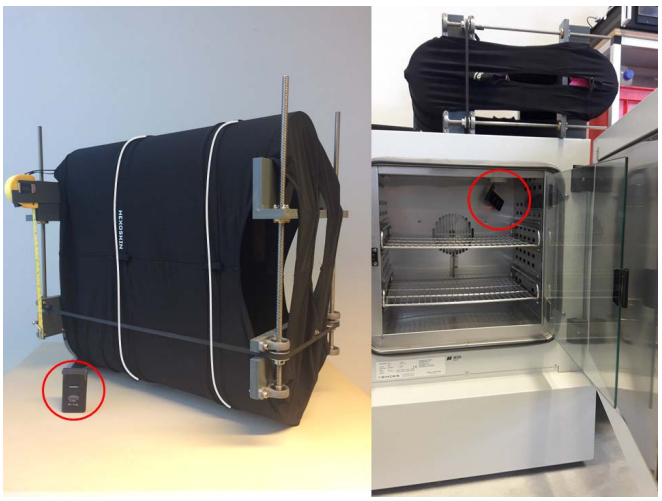

Fig. 2. (Left) Hexoskin on torso model, with white lines indicating RIP in the Hexoskin, and the device appearing in the red circle. (Right) Hexoskin on torso model during temperature test, the torso model is placed in a climate-control chamber, into which, the device can be inserted (see red circle).

### B. Torso Model

To simulate changes in thoracic and abdominal circumference, a custom-made torso model was constructed (see Fig. 2). The model made of two half cylinders, which could be moved manually towards or away from each other. A tape measure was used to determine the distance between the cylinder halves and the corresponding circumference was calculated. In this model, the change was equal for both the thoracic band and the abdominal band.

### C. Temperature-Output Measurement

Two shirts (M3XL, M4XL) were used to study the relationship between temperature and the thoracic and abdominal output. A small climate-controlled chamber (Kühlinkubator Modell KB53, Binder, Tuttlingen, Germany) was used to increase and decrease temperature to a preset value. The device was inserted into the climate-controlled chamber through an opening for cables (see Fig. 2). Temperature was increased from room temperature to a maximum of 42 degrees Celsius, and then decreased again. The circumference of the Hexoskin was kept constant during all 15 of these temperature tests. The starting and ending temperatures were different for each measurement, however all temperatures lay between 20-45 degrees Celsius. The length of the measurement depended on the temperature rise or fall in the measurement. Therefore, all 15 measurement were different in length.

### D. Circumference-Output Measurement

All shirts were used to investigate the relationship between thoracic and abdominal circumference and the output. The minimum and maximum circumference for every variant of the shirt are given in Table I. In five equal steps, the circumference

of the model was increased, and in another series of five steps, decreased all within the given range. Each step was maintained for 1 minute. In supplemental S1, a detailed protocol can be found which describes how the steps were derived per shirt size. The temperature in the room was kept constant during these tests. After all circumferences had been tested, the shirt was removed from the model, disconnected and reapplied to the model. A second test was performed for each shirt, resulting in a total of 24 tests.

### E. Signal Analysis

The data from all measurements were retrieved from the device by connecting it to a computer. The signals were processed in MATLAB 2018a (MathWorks). All measurements contained time, thoracic output and abdominal output, and temperature arrays. All data was sampled with a sample frequency of 128 Hz. No pre-processing of the data was performed, accept for filtering the temperature data with a Savitsky-Golay filter.

*1) Temperature-Output Relationship:* In this part of the analysis, time, temperature, thoracic and abdominal output were used from the data. Thoracic or abdominal output was plotted against the temperature data. A linear relationship was selected as an initial approximation for the relationship between temperature and output. The temperature-output relationship was established with least squares regression for both the thoracic (2a) and abdominal band (2b). The temperature was measured in the device and used as input for both the thoracic and abdominal signal. In (2a) and (2b), $\text{output}_{\text{TH}}$ and $\text{output}_{\text{ABD}}$ are presented in AU, temperature is presented in degrees Celsius (°C), $\text{slope}_{\text{THTEMP}}$ and $\text{slope}_{\text{ABDTEMP}}$ are presented in AU/°C. A temperature correction equation was formulated, see (2c) and (2d). In (2c) and (2d), $\text{output}_{\text{THcorr}}$ and $\text{output}_{\text{ABDcorr}}$ are presented in AU, temperature relative to start temperature is presented in degrees Celsius (°C), $\text{slope}_{\text{THTEMP}}$ and $\text{slope}_{\text{ABDTEMP}}$ are in AU/°C. The output has been corrected for temperature changes.

$$output_{TH} = slope_{THTEMP}\ temperature \tag{2a}$$

$$output_{ABD} = slope_{ABDTEMP}\ temperature \tag{2b}$$

$$output_{THcorr} = output_{TH} - slope_{THTEMP}(temperature - temperature\,(t_0)) \tag{2c}$$

$$output_{ABDcorr} = output_{ABD} - slope_{ABDTEMP} \times (temperature - temperature\,(t_0)) \tag{2d}$$

After the application of the temperature correction, $\text{slope}_{\text{THTEMPcorr}}$ and $\text{slope}_{\text{ABDTEMPcorr}}$ were determined, as given in (2e) and (2f).

$$output_{THcorr} = slope_{THTEMPcorr}\ temperature \tag{2e}$$

$$output_{ABDcorr} = slope_{THTEMPcorr}\ temperature \tag{2f}$$

To obtain a clinical insight into the feasibility of using the smart shirt to measure DH and SH, we calculated the drift due to one degree of temperature change before and after temperature correction. We applied a linear function to calibrate the output to volume, see (3a) and (3b). Because the thoracic and abdominal band utilize different base frequencies, a factor must be applied in order to get equal values for the two bands. The thoracic and abdominal band operate at respectively frequencies of 26MHz and 16MHz. Therefore, the abdominal signal is multiplied with factor 1.625 (26/16). The drift in mL/°C was determined by summing the values for $\text{slope}_{\text{THTEMP}}$ and $\text{slope}_{\text{ABDTEMP}}$ and applying an average (spirometric-based) calibration factor derived from healthy subjects (1 AU = 7 mL). The same procedure was followed for the temperature corrected output.

$$drift = 7\left(slope_{THTEMP} + 1.625 * slope_{ABDTEMP}\right) \tag{3a}$$

$$drift_{corr} = 7\left(slope_{THTEMPcorr} + 1.625 * slope_{ABDTEMPcorr}\right) \tag{3b}$$

*2) Circumference-Output Relationship:* In this part of the analysis, time, thoracic and abdominal output were used from the data. As described earlier, a circumference step was maintained for a minute. The mean value of thoracic output and abdominal output was determined from this time window. Given that the relationship between circumference and output was expected to be linear, we used least squares regression to determine linear approximation, see (4a) and (4b). In which $\text{output}_{\text{TH}}$ and $\text{output}_{\text{ABD}}$ are presented in AU, circumferenceTH and $\text{circumference}_{\text{ABD}}$ are presented in cm, $\text{slope}_{\text{TH}}$ and $\text{slope}_{\text{ABD}}$ is presented in AU/cm. The $R^2$ of fitted linear data were calculated using the raw data was.

$$output_{TH} = slope_{TH}\ circumference_{TH} \tag{4a}$$

$$output_{ABD} = slope_{ABD}\ circumference_{ABD} \tag{4b}$$

## III. Results

### A. Temperature-Output Relationship

The output response to temperature changes was tested in 15 measurements. The measurements had a mean duration of 19.5 (9.3) minutes. On average the minimum temperature was 26.9 (8.3) °C and the maximum temperature was 36.6 (9.9) °C. Temperature was plotted against thoracic and abdominal output. The results reveal a linear relation between temperature and output (the fits of the derived thoracic and abdominal equation were $R^2 > 0.97$ and $R^2 > 0.87$, respectively). An example of the relationship between temperature and output is presented in Fig. 3, in addition the fitted data is given as a dotted line.

Based on the linear regression of the data, we found $\text{slope}_{\text{THTEMP}}$ and $\text{slope}_{\text{ABDTEMP}}$, according to (2a) and (2b). The median (interquartile range; IQR) $\text{slope}_{\text{THTEMP}}$ is −3.23 (−3.42; −3.19) AU/°C and the median $\text{slope}_{\text{ABDTEMP}}$ is −1.06 (−1.21; −0.9) AU/°C over all measurements. By substitution of $\text{slope}_{\text{THTEMP}}$ and $\text{slope}_{\text{ABDTEMP}}$ in (2c) and (2d), the corrected signals could be derived. As calculated from (2e) and (2f), the median (IQR) $\text{slope}_{\text{THTEMPcorr}}$ is 0.0014 (−0.19;0.04) AU/°C and the median $\text{slope}_{\text{ABDTEMPcorr}}$ is 0.0035 (−0.15; 0.16) AU/°C over all measurements. Temperature over time is displayed in the upper part of Fig. 4,

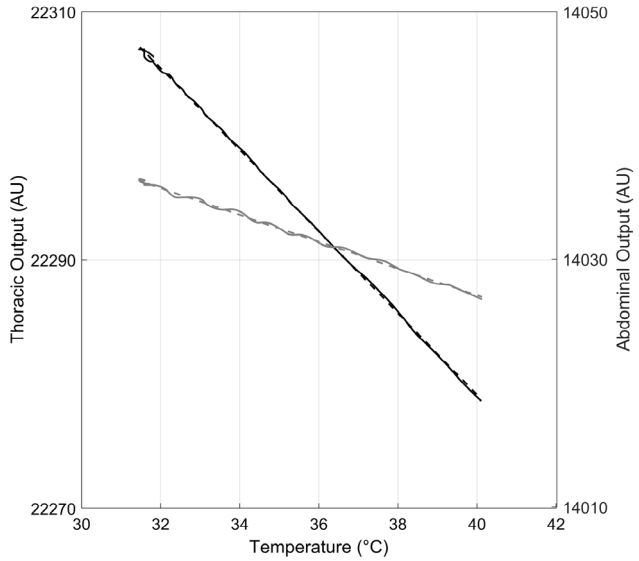


Fig. 3. Example of relationship between thoracic and abdominal output (AU) and temperature (°C). Thoracic output (black solid line) is indicated along the left y-axis, with the right y-axis indicating abdominal output (gray solid line). As can be seen from the figure, a linear relation exists between temperature and the output of both straps. With least squares the relationship was derived a fitted data is displayed in the figure as dotted lines.

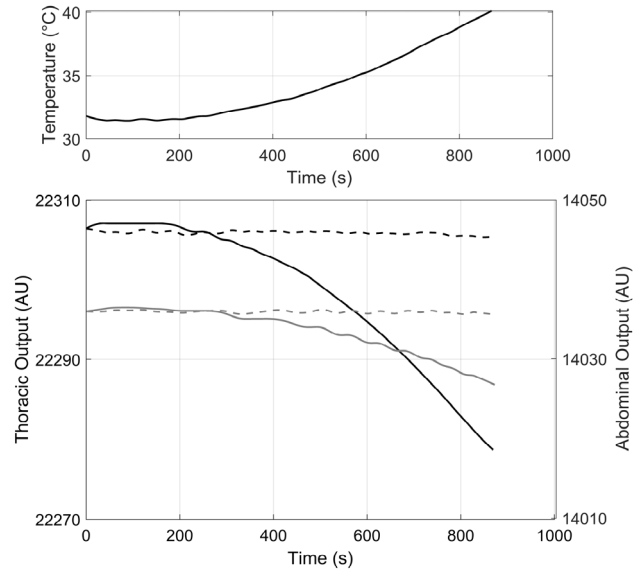


Fig. 4. Example of a temperature measurement. The upper chart displays temperature (°C) of the device over time (s), as a result of the temperature increase in the climate-controlled chamber. In the lower chart, the output as a result of the changes in temperature can be found. The thoracic and abdominal uncorrected output are represented by the solid black and grey line respectively. After the temperature correction is performed the output shows less temperature dependency and displayed as the dashed lines. Thoracic output and abdominal output are displayed along the left and right y-axes, respectively. Time is displayed in seconds and both thoracic and abdominal output in arbitrary units.

with output over time for both the corrected and uncorrected signals displayed in the lower part.

The median drift in mL as a function of temperature, as calculated with (3a) and (3b), is −34.7 mL/°C and the median $\text{drift}_{\text{corr}}$ is −0.50 mL/°C.

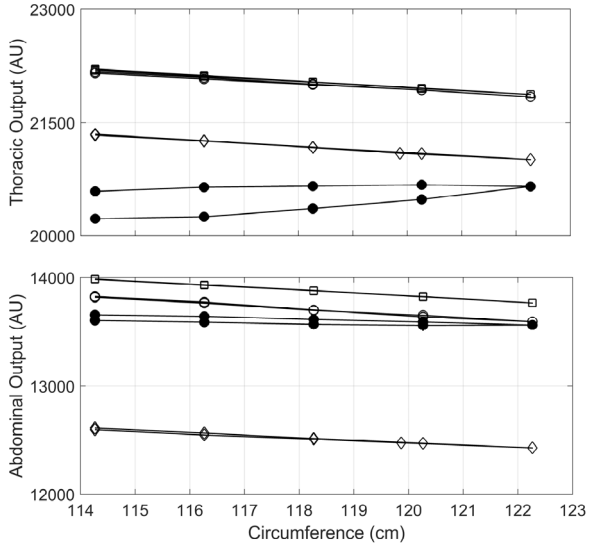


Fig. 5. Example circumference-output relationship for four M3XL shirts. In the measurement, circumference was increased and decreased in a total of 10 steps (represented by the markers). Circumference (cm) is displayed along the x-axis, with the y-axis representing the output (AU) of the thoracic band (upper chart) and abdominal band (lower chart). Three 3XL shirts (represented by diamonds, squares, and open circles) exhibit a linear relationship between circumference and output, whereas one 3XL shirt (solid circles) is nonlinear, with the greatest nonlinearity occurring in the thoracic band.

### B. Circumference-Output Relation

The output response to five different circumferences (see supplemental S1) were determined for all 12 shirts. Per step in circumference the mean output was determined, which was plotted against that circumference. 9 out of 12 shirts showed a linear output to the changes in circumference. The other shirts (M4XL (2), M3XL (1)) showed a nonlinear nonreproducible circumference-output relation (see Fig. 5). The measurements taken with the non-linear shirts were excluded from further analysis. With least squares regression the slope of the linear relation was determined, see (4a) and (4b). The median (IQR) $\text{slope}_{\text{TH}}$ measured is −40.2 (−42.7; −36.5) AU/cm, and the median (IQR) $\text{slope}_{\text{ABD}}$ is −22.8 (−27.3; −21.3) AU/cm. The fit of the derived linear data to the measured data was $R^2 > 0.89$ for both the thoracic and the abdominal data.

## IV. Discussion

RIP technology shows drift under the influence of temperature changes correcting for this allows the shirt to take volume measurement (e.g. hyperinflation). The smart shirt used in this study has proven to have a linear temperature dependency. Changes in the temperature of the device containing the oscillator generated a volume drift of −34.7 mL/°C. The drift could be corrected using a temperature correction function, resulting in remaining drift of only −0.50 mL/°C. Moreover, the relationship between circumference and output was linear in 9 out of 12 shirts.

### A. Temperature-Output Relationship

The central frequency of an oscillator circuit is known to change over time in response to temperature changes [53].

Likewise, measured with the same circuit, physiological drifts, (i.e. SH and DH), are also characterized by change in central frequency. To distinguish between these two drifts, we examined the relationship between temperature and RIP output. In earlier pilot studies, we confirmed that the drift originated from changes in the temperature of the device, and not from changes in the temperature of the thoracic and abdominal band. The results of the current study indicate that temperature drift can be minimized by a simple linear function. Median (IQR) $\text{slope}_{\text{THTEMP}}$ is $-3.23$ ($-3.42$; $-3.19$) AU/°C and median $\text{slope}_{\text{ABDTEMP}}$ is $-1.06$ ($-1.21$; $-0.9$) AU/°C over all measurements.

This study is the first to quantify temperature dependency on a thorax model. To the best of our knowledge, existing literature contains only one study testing the stability of RIP signals. In 1988, Watson *et al.* [55] evaluated the stability of the Respitrace RIP system baseline over a period of 12 hours. They found no significant baseline drift and attributed this to the use of a thermally compensated oscillator module. We used a digital solution to compensate for temperature drift but an analog approach would have also worked. Both methods demonstrated that signals from RIP can be stabilized. Our results are in line with those reported by Neumann *et al.* [51], and Leino *et al.* [52]. Neumann *et al.* studied induced changes in lung volume and observed a drift in lung volume. They suggested that the observed drift could be explained by the increase in body temperature seen in patients admitted to the ICU. Likewise, Leino *et al.* [52] describe a drift in RIP signals (Respitrace) due to thermal instability, which affected the results when measuring FRC in subjects with acute lung injury. These results appear to be in contrast with the study of Watson *et al.* however, they reported that the earlier versions of the Respitrace were not thermally stabilized. The non-stabilized Respitrace may have been used in that study. Another explanation could be that the temperature changes in the first study were smaller than those in the latter, resulting in differences in baseline drifts. In contrast to our results, Sackner *et al.* [70] tested RIP prior to measurements and concluded that the changes that they observed in FRC cannot be explained by temperature changes. They reported that the room temperature had not changed during the measurements, but they did not take changes in body temperature into account.

### B. Circumference-Output Relation

The majority of shirts (9 of 12) showed a linear relation in the output to a change in circumference. For three shirts, M3XL (1) and M4XL (2), we found a nonlinear relationship between input and output. Measurements with these shirts were performed again, resulting in a non-reproducible, nonlinear relationship. The relationships derived in the two measurements using the same device were not comparable. This suggests that the problem is in the shirts, and not in the device. The cause remains unknown.

Watson *et al.* [55] determined a linear and second-order polynomial function between the cross-sectional area of a curved or squared object and RIP output. They found $R^2$values of 99.16%, 98.92%, 99.95% and 99.54% respectively for the second-order and linear functions of the curved object, and for the second-order and linear functions of the squared object. The $R^2$ values for both shapes were only slightly better for the second-order polynomial function. Zhang *et al.* [57] developed their own RIP system and tested the linearity of their sensors on a chest wall model. In the model, which was similar to the model we used, circumference and cross-sectional area could be derived based on the distance between the two halves of the model. The relationship between cross-sectional area and the output of the RIP system was determined, revealing a strong linear relationship ($R^2$: 0.99). In our model we found an $R^2 >$ 0.89 but the circumference was harder to control, especially in the smaller shirt sizes. This led to some small discrepancies in the data, resulting in $R^2$ values slightly lower than those reported by Watson *et al.* and Zhang *et al.* In contrast to the current study on the relationship between circumference and output, Watson *et al.* and Zhang *et al.* studied the relation between cross-sectional area and the output. We opted to use circumference as input given the supposed linear relationship between circumference and to lung volume [42]. Our results are nevertheless in agreement, as the change in circumference of our model has a close to constant proportional relation to the change in cross-sectional area. While the largest change in circumference was observed in the M4XL shirt (15 cm in total), the ratio between circumference and cross-sectional area remained limited (varying between 0.153 and 0.156).

### C. Clinical Implications

DH is defined as a change in FRC of 150 ml over exercise [26], [31]. In contrast, there is no standardized classification system for the assessment of severity of SH [71]. To the best of our knowledge, the literature only contains two studies [51], [52] investigating the use of RIP technology to measure lung inflation. Leino *et al.* [52] concludes that it is possible to monitor acute changes in lung inflation. Long-term measurement is not possible, however, due to considerable baseline drift. Which can be attributed in part to thermal instability. Although the effect of temperature is not examined exclusively, baseline drift is defined in both studies. Neumann *et al.* and Leino *et al.* report a drift of 25 mL/min and 8 mL/min respectively. Within a maximum of 20 minutes, a patient could be scored as a hyperinflator. We hypothesized that the temperature fluctuations occurring during these measurements were small, given that the measurements took place in controlled conditions. This might indicate that the volume drift could be considerably larger under noncontrolled conditions, as is the case during home monitoring. For this reason, we established the relationship between temperature and output. According to our results, without a temperature correction, a subject could be classified as a hyperinflator when temperature changes with approximately 4.3°C (∼150 mL). It is known that skin temperature can fall multiple degrees with exercise [72]. The chance of a false diagnosis of DH increases even more for subjects with FRC changes between 0 and 150 mL. In the corrected signals, the influence of temperature changes on the measured volume are negligible. Per °C, the volume drift was only $-0.50$ mL. This means that, in the corrected signals, the same temperature change (4.3°C) increases the measured FRC by only 2.2 mL.

The smart shirt is therefore a feasible method for measuring SH and DH, provided that a temperature correction is performed.

As mentioned in the introduction, there is a linear relationship between circumference of the thorax and abdomen. In earlier studies [44], [73], linear calibration has been used to determine the breathing patterns of subjects. To be able to use a linear function to calibrate the output of RIP to lung volumes, the relationship between input and output of the shirt should also be linear. We found a linear relationship between the circumference and the output of the shirt. A linear function may therefore be used to calibrate the output of the shirt (in AU) to volume.

The thermal stability (after correction) and linearity of the sensors established in this study suggest that this smart shirt is a promising tool for home monitoring. It is easily worn by patients eliminating concerns about disturbing the measurements during their normal activities in and around the house.

### D. Limitations

The relationship between temperature and output were not examined during changes in circumference or with different rates of temperature change. One limitation in this study is that the torso model was operated manually. This made the circumference harder to control, especially for small shirt sizes. This could have caused minor discrepancies in the calculations. Our protocol did not include repeated increases and decreases in circumference. In a small pilot study conducted prior to the measurements taken in this research, however, we determined that the manually operated model is a reproducible method for deriving the relationship between circumference and output (coefficient of variation $< 0.04$).

## V. Conclusion

Respiratory inductance plethysmography (RIP) is a feasible method for measuring lung volumes (e.g. DH and SH), provided that a temperature correction is performed, and the circumference-output relationship is linear. A linear function can be used to correct for temperature dependent drift in the thoracic and abdominal output of the shirt. The majority of the shirts tested in this study, show a linear relationship between circumference and output. We intend to validate the measurement of lung hyperinflation with the Hexoskin in healthy subjects and COPD patients. After comparison to a clinical standard, a clinical trial at home will be set up. This trial will give us an insight in the day-to-day variation in lung hyperinflation, and its connection to symptoms experienced by patients. Moreover, we will try to define exacerbation prediction models with artificial intelligence based on the signals of the Hexoskin, including the inflation status of the lungs.

## Acknowledgment

The authors would like to thank J.W. van Dongen for contributing to the project and helping with data acquisition.

## References

[1] *Global Strategy for the Diagnosis, Management, and Prevention of COPD*. Accessed: Dec. 3, 2019. [Online]. Available: www.goldcopd.org

[2] S. Baraldo, G. Turato, and M. Saetta, "Pathophysiology of the small airways in chronic obstructive pulmonary disease," *Respiration*, vol. 84, no. 2, pp. 89–97, 2012.

[3] J. Cruz and D. A. B. Marques, "Home telemonitoring effectiveness in COPD: A systematic review," *Int. J. Clin. Pract.* vol. 68, no. 3, pp. 369–378, 2014.

[4] I. Tomasic, N. Tomasic, R. Trobec, M. Krpan, and T. Kelava, "Continuous remote monitoring of COPD patients—Justification and explanation of the requirements and a survey of the available technologies," *Med. Biol. Eng. Comput.*, vol. 56, no. 4, pp. 547–569, Apr. 2018.

[5] G. T. Ferguson, "Why does the lung hyperinflate?" *Proc. Amer. Thorac. Soc.*, vol. 3, no. 2, pp. –176–179, 2006.

[6] A. M. Yohannes, "Management of dyspnea and anxiety in chronic obstructive pulmonary disease: A critical review," *J. Amer. Med. Directors Assoc.*, vol. 18, no. 12, 2016, Art. no. 1096.

[7] A. H. Sodhro, S. Pirbhulal, G. H. Sodhro, A. Gurtov, M. Muzammal, and Z. Luo, "A joint transmission power control and duty-cycle approach for smart healthcare system," *IEEE Sensors J.*, vol. 19, no. 19, pp. 8479–8486, Oct. 2019.

[8] N. Cherif, Y. Ouakrim, A. Benazza-Benyahia, and N. Mezghani, "Physical activity classification using a smart textile," in *Proc. IEEE Life Sci. Conf. (LSC)*, Oct. 2018, pp. 175–178.

[9] W. Wu, H. Zhang, S. Pirbhulal, S. C. Mukhopadhyay, and Y.-T. Zhang, "Assessment of biofeedback training for emotion management through wearable textile physiological monitoring system," *IEEE Sensors J.*, vol. 15, no. 12, pp. 7087–7095, Dec. 2015.

[10] T. Zhang *et al.*, "A joint deep learning and Internet of medical things driven framework for elderly patients," *IEEE Access*, vol. 8, pp. 75822–75832, 2020.

[11] L. Gonzales, "Textile sensor system for electrocardiogram monitoring," in *Proc. IEEE Virtual Conf. Appl. Commercial Sensors (VCACS)*. Mar. 2015, pp. 1–4.

[12] M. Roudjane *et al.*, "Smart T-shirt based on wireless communication spiral fiber sensor array for real-time breath monitoring: Validation of the technology," *IEEE Sensors J.*, early access, May 8, 2020, doi: 10.1109/JSEN.2020.2993286.

[13] J. D. Jonckheere, "OFSETH: Smart medical textile for continuous monitoring of respiratory motions under magnetic resonance imaging," in *Proc. Annu. Int. Conf. IEEE Eng. Med. Biol. Soc.*, Sep. 2009, pp. 1473–1476.

[14] W. Wu, S. Pirbhulal, H. Zhang, and S. C. Mukhopadhyay, "Quantitative assessment for self-tracking of acute stress based on triangulation principle in a wearable sensor system," *IEEE J. Biomed. Health Informat.*, vol. 23, no. 2, pp. 703–713, Mar. 2019.

[15] M. Ghahremani Honarvar and M. Latifi, "Overview of wearable electronics and smart textiles," *J. Textile Inst.*, vol. 108, no. 4, pp. 631–652, Apr. 2017.

[16] R. Paradiso, T. Faetti, and S. Werner, "Wearable monitoring systems for psychological and physiological state assessment in a naturalistic environment," in *Proc. Annu. Int. Conf. IEEE Eng. Med. Biol. Soc.*, Aug. 2011, pp. 2250–2253.

[17] K. M. B. Jansen, "Smart textiles: How electronics merge into our clothing," in *Proc. Int. Conf. Thermal*, Mar. 2019, pp. 1–4.

[18] A. Lenferink *et al.*, "Self-management interventions including action plans for exacerbations versus usual care in patients with chronic obstructive pulmonary disease," *Cochrane Database Systematic Rev.*, vol. 8, Aug. 201, Art. no. Cd011682.

[19] L. Boer *et al.*, "Validation of ACCESS: An automated tool to support self-management of COPD exacerbations," *Int. J. Chronic Obstructive Pulmonary Disease*, vol. 13, pp. 3255–3267, Oct. 2018.

[20] A. Stenzler, "Inspiratory capacity: The key to home monitoring patients with COPD," *Respiratory Therapy*, vol. 12, no. 4, p. 15, 2017.

[21] A. Madueño, "Usefulness of inspiratory capacity measurement in COPD patients in the primary care setting," *Int. J. Gen. Med.*, vol. 2, pp. 219–225, Oct. 2009.

[22] D. E. O'Donnell and M. K. A. Lam Webb, "Measurement of symptoms, lung hyperinflation, and endurance during exercise in chronic obstructive pulmonary disease," *Amer. J. Respiratory Crit. Care Med.*, vol. 158, no. 1, pp. 1557–1565, 1998.

[23] C. C. Bellos, A. Papadopoulos, R. Rosso, and D. I. Fotiadis, "Identification of COPD Patients' health status using an intelligent system in the CHRONIOUS wearable platform," *IEEE J. Biomed. Health Informat.*, vol. 18, no. 3, pp. 731–738, May 2014.

[24] P. P. Walker, "Telemonitoring in chronic obstructive pulmonary disease (CHROMED). A randomized clinical trial," *Amer. J. Respiratory Crit. Care Med.*, vol. 198, no. 5, pp. 620–628, 2018.

[25] C. Esteban *et al.*, "Outcomes of a telemonitoring-based program (telEPOC) in frequently hospitalized COPD patients," *Int. J. Chronic Obstructive Pulmonary Disease*, vol. 11, pp. 2919–2930, Nov. 2016.

[26] D. E. O'Donnell and S. M. K. A. Revill Webb, "Dynamic hyperinflation and exercise intolerance in chronic obstructive pulmonary disease," *Amer. J. Respiratory Crit. Care Med.*, vol. 164, no. 5, pp. 770–777, 2001.

[27] P. Gagnon, "Pathogenesis of hyperinflation in chronic obstructive pulmonary disease," *Int. J. Chronic Obstructive Pulmonary Disease*, vol. 9, pp. 187–201, Oct. 2014.

[28] J. B. West, *Respiratory Physiology: The Essentials*. Philadelphia, PA, USA: Lippincott Williams & Wilkins, 2012.

[29] T. G. Liou and R. E. Kanner, "Measurement of lung volumes," *Clin. Rev. Allergy Immunol.*, vol. 37, no. 3, pp. 153–158, 2009.

[30] D. Mannee, "Is the metronome-paced tachypnea test (MPT) ready for clinical use? Accuracy of the MPT in a prospective and clinical study," *Respiration*, vol. 97, no. 6, pp. 569–575, 2019.

[31] A. Benfante, F. Di Marco, S. Terraneo, S. Centanni, and N. Scichilone, "Dynamic hyperinflation during the 6-min walk test in severely asthmatic subjects," *ERJ Open Res.*, vol. 4, no. 2, p. 143, Apr. 2018.

[32] D. E. O'Donnell, K. A. Webb, and J. A. Neder, "Lung hyperinflation in COPD: Applying physiology to clinical practice," *COPD Res. Pract.*, vol. 1, no. 1, pp. 1–5, Dec. 2015.

[33] K. Klooster, N. H. T. ten Hacken, J. E. Hartman, F. C. Sciurba, H. A. M. Kerstjens, and D.-J. Slebos, "Determining the role of dynamic hyperinflation in patients with severe chronic obstructive pulmonary disease," *Respiration*, vol. 90, no. 4, pp. 306–313, Oct. 2015.

[34] J. Varga, "Mechanisms to dyspnoea and dynamic hyperinflation related exercise intolerance in COPD," *Acta Physiol. Hung*, vol. 102, no. 2, pp. 75–163, 2015.

[35] A. Rossi *et al.*, "Mechanisms, assessment and therapeutic implications of lung hyperinflation in COPD," *Respiratory Med.*, vol. 109, no. 7, pp. 785–802, Jul. 2015.

[36] M. I. Soffler, M. M. Hayes, and R. M. Schwartzstein, "Respiratory sensations in dynamic hyperinflation: Physiological and clinical applications," *Respiratory Care*, vol. 62, no. 9, pp. 1212–1223, Sep. 2017.

[37] P. M. A. Calverley and N. G. Koulouris, "Flow limitation and dynamic hyperinflation: Key concepts in modern respiratory physiology," *Eur. Respiratory J.*, vol. 25, no. 1, p. 186, 2005.

[38] M. R. Miller, "Standardisation of spirometry," *Eur. Respiratory J.*, vol. 26, no. 2, pp. 319–338, Aug. 2005.

[39] J. A. Adams, "Tidal volume measurements in newborns using respiratory inductive plethysmography," *Amer. Rev. Respir. District*, vol. 148, no. 3, pp. 585–588, 1993.

[40] R. D. Ballard, P. L. Kelly, and R. J. Martin, "Estimates of ventilation from inductance plethysmography in sleeping asthmatic patients," *Chest*, vol. 93, no. 1, pp. 128–133, Jan. 1988.

[41] C. Dadzie and M. M. H. Simpser Lavietes, "Measurement of tidal breath by determination of chest wall volume displacement in patients with airflow obstruction," *Chest*, vol. 88, no. 3, pp. 420–425, 1985.

[42] K. Konno and J. Mead, "Measurement of the separate volume changes of rib cage and abdomen during breathing," *J. Appl. Physiol.*, vol. 22, no. 3, pp. 407–422, 1967.

[43] C. F. Clarenbach, "Monitoring of ventilation during exercise by a portable respiratory inductive plethysmograph," *Chest*, vol. 128, no. 3, pp. 1282–1290, 2005.

[44] C. Heyde, "Respiratory inductance plethysmography-a rationale for validity during exercise," *Med. Sci. Sports Exerc.*, vol. 46, no. 3, pp. 488–495, 2014.

[45] H. Leutheuser, C. Heyde, K. Roecker, A. Gollhofer, and B. M. Eskofier, "Reference-free adjustment of respiratory inductance plethysmography for measurements during physical exercise," *IEEE Trans. Biomed. Eng.*, vol. 64, no. 12, pp. 2836–2846, Dec. 2017.

[46] D. Kogan, A. Jain, S. Kimbro, G. Gutierrez, and V. Jain, "Respiratory inductance plethysmography improved diagnostic sensitivity and specificity of obstructive sleep apnea," *Respiratory Care*, vol. 61, no. 8, pp. 1033–1037, Aug. 2016.

[47] J. L. Werchowski, "Inductance plethysmography measurement of CPAP-induced changes in end-expiratory lung volume" *J. Appl. Physiol.*, vol. 68, no. 4, pp. 1732–1738, 1990.

[48] J. H. Atkins, "A pilot study of respiratory inductance plethysmography as a safe, noninvasive detector of jet ventilation under general anesthesia," *Anesth Analg.*, vol. 111, no. 5, pp. 1168–1175, 2010.

[49] Y. Retory, P. Niedzialkowski, C. de Picciotto, M. Bonay, and M. Petitjean, "New respiratory inductive plethysmography (RIP) method for evaluating ventilatory adaptation during mild physical activities," *PLoS ONE*, vol. 11, no. 3, Mar. 2016, Art. no. e0151983.

[50] K. P. Cohen, "Comparison of impedance and inductance ventilation sensors on adults during breathing, motion, and simulated airway obstruction," *IEEE Trans. Biomed. Eng.*, vol. 44, no. 7, pp. 555–566, Jul. 1997.

[51] P. Neumann, "Evaluation of respiratory inductive plethysmography: Accuracy for analysis of respiratory waveforms," *Chest*, vol. 113, no. 2, pp. 443–451, 1998.

[52] K. Leino, "Validation of a new respiratory inductive plethysmograph," *Acta Anaesthesiol Scand*, vol. 45, no. 1, pp. 101–104, 2001.

[53] R. Rhea, *Oscillator Design and Computer Simulation*. London, U.K.: The Institution of Engineering and Technology, 1995.

[54] U. Denier, "Analysis and design of an ultralow-power CMOS relaxation oscillator," *IEEE Trans. Circuits Syst. I, Reg. Papers*, vol. 57, no. 8, pp. 1973–1982, Aug. 2010.

[55] H. L. Watson and D. A. M. A. Poole Sackner, "Accuracy of respiratory inductive plethysmographic cross-sectional areas," *J. Appl. Physiol.*, vol. 65, no. 1, pp. 306–308, 1980.

[56] J. A. Barnes, "Characterization of frequency stability," *IEEE Trans. Instrum. Meas.*, vol. IM-20, no. 2, pp. 105–120, May 1971.

[57] Z. Zhang, J. Zheng, H. Wu, W. Wang, B. Wang, and H. Liu, "Development of a respiratory inductive plethysmography module supporting multiple sensors for wearable systems," *Sensors*, vol. 12, no. 10, pp. 13167–13184, Sep. 2012.

[58] K. P. Cohen, D. Panescu, J. H. Booske, J. G. Webster, and W. J. Tompkins, "Design of an inductive plethysmograph for ventilation measurement," *Physiol. Meas.*, vol. 15, no. 2, pp. 217–229, May 1994.

[59] A. S. Sedra, *Microelectronic Circuits*. London, U.K.: Oxford Univ. Press, 2016.

[60] R. Corriveau, *Wearable Respiratory Inductance Plethysmography Device and Method for Respiratory Activity Analysis*. Montreal, QC, Canada: Carre Technologies, 2015.

[61] R. Corriveau, "Low-power respiratory inductance plethysmography device, intelligent garments or wearable items equipped therewith and a method for respiratory activity analysis," Carré Technol., Montreal, QC, Canada, Tech. Rep. CA2896498C, 2014.

[62] P. A. Fournier, "Washable intelligent garment and components thereof," Carré Technol., Montreal, QC, Canada, Tech. Rep. WO2013134856A1, 2013.

[63] M. B. Phillips, "Reliability and validity of the Hexoskin wearable body metrics telemetry shirt," *J. Sport Hum. Perform.*, vol. 5, no. 2, p. 151, 2017.

[64] C. A. Elliot, M. J. Hamlin, and C. A. Lizamore, "Validity and reliability of the hexoskin wearable biometric vest during maximal aerobic power testing in elite cyclists," *J. Strength Conditioning Res.*, vol. 33, no. 5, pp. 1437–1444, May 2019.

[65] R. Villar and T. R. L. B. Hughson, "Validation of the Hexoskin wearable vest during lying, sitting, standing, and walking activities," *Appl. Physiol. Nutr Metab*, vol. 40, no. 10, pp. 1019–1024, 2015.

[66] T. Beltrame, R. Amelard, A. Wong, and R. L. Hughson, "Prediction of oxygen uptake dynamics by machine learning analysis of wearable sensors during activities of daily living," *Sci. Rep.*, vol. 7, no. 1, p. 45738, May 2017.

[67] T. Banerjee, "Evaluating a potential commercial tool for healthcare application for people with dementia," in *Proc. Int. Conf. Health Inform. Med. Syst.*, Las Vegas, NV, USA, 2015, pp. 1–4.

[68] C. Al Sayed, L. Vinches, and S. Hallé, "Validation of a wearable biometric System's ability to monitor heart rate in two different climate conditions under variable physical activities," *E-Health Telecommun. Syst. Netw.*, vol. 6, no. 2, pp. 19–30, 2017.

[69] *Size Chart*. Accessed: Dec. 1, 2018. [Online]. Available: https://cdn.shopify.com/s/files/1/0284/7802/t/52/assets/SC19-Men_Sizing.png?v=5575764245896454804

[70] M. A. Sackner, "Calibration of respiratory inductive plethysmograph during natural breathing," *J. Appl. Physiol.*, vol. 66, no. 1, pp. 410–420, 1989.

[71] D. E. O'Donnell and P. Laveneziana, "Physiology and consequences of lung hyperinflation in COPD," *Eur. Respiratory Rev.*, vol. 15, no. 100, pp. 61–67, Dec. 2006.
[72] M. Torii, M. Yamasaki, T. Sasaki, and H. Nakayama, "Fall in skin temperature of exercising man.," *Brit. J. Sports Med.*, vol. 26, no. 1, pp. 29–32, Mar. 1992.
[73] P. Y. Carry, "Evaluation of respiratory inductive plethysmography: Accuracy for analysis of respiratory waveforms," *Chest*, vol. 111, no. 4, pp. 910–915, 1997.

**Denise Mannée** was born in Amersfoort, Utrecht, The Netherlands, in 1992. She received the B.S. and M.S. degrees in technical medicine from the University of Twente in 2013 and 2017, respectively. She is currently pursuing the Ph.D. degree in medicine with the Radboud University Medical Centre, Nijmegen, The Netherlands.

Since 2017, she was a Junior Researcher with the Radboud University Medical Centre. Her research interests include lung physiology, the development of home monitoring devices, and improvement of care for patient with chronic pulmonary disease.

Prof. Mannée was a recipient of the ERS Young Scientist Sponsorship 2019.

**Hanneke van Helvoort** received the M.S. degree in biomedical sciences and the Ph.D. degree in medical sciences from Radboud University, Nijmegen, The Netherlands, in 2002 and 2006, respectively.

As a Senior Researcher, she is currently working on optimizing or innovating diagnostics for lung patients. This reflects the main focus of her work, thereby contributing to the characterization and therapeutic evaluations for patients. Her research interests include lung physiology and immunology. Dr. van Helvoort was a member of the Junior Members Committee, the European Respiratory Society from 2013 to 2016. Within The Netherlands, she has been involving in the national educational program for pulmonary function technicians since 2006.

**Frans de Jongh** was born in the South of The Netherlands, in 1963. He received the B.S. and M.S. degrees in aerospace engineering from the Delft University of Technology, The Netherlands, in 1987, and the Ph.D. degree from the Department of Neonatal Intensive Care, University of Amsterdam, and the Group of Theoretical Aerodynamics, Aerospace Engineering, Delft University of Technology in 1995.

His thesis was titled Ventilation Modeling of the Human Lung. After that, he became an Assistant Professor in Delft (Bio Fluid Dymamics) and a Scientific Researcher with the Neonatal Intensive Care, AMC University Hospital, Amsterdam. In 2001, he switched his position from Delft to the University of Enschede, Mechanical Engineering, Department of Engineering Fluid Dynamics, and also became the Head of the Pulmonary Function Laboratory, Department of Pulmonology, MST Hospital, Enschede, The Netherlands. He is the author of over 65 peer-reviewed articles and several book chapters all related to pulmonology and technology. His research interests include lung function measurements from premature neonate to elderly, breathing spontaneously till any form of respiratory support, including all kinds of mechanical ventilation. Developing and testing new devices in this field are his key interest but he also works in the field of medical aerosols and electronic nose research.

Dr. de Jongh was a Secretary and the Head of Assembly 9 (the Allied Health Professionals) of the European Respiratory Society (the ERS), the co-chaired several worldwide task forces (ERS/ATS and ERS/ISAM), and the Director of E-learning of the ERS. He received the price as a Best Teacher of the University Twente.